

Heisenberg-Limited Quantum Metrology without Ancilla

Qiushi Liu^{*} and Yuxiang Yang[†]

*QICI Quantum Information and Computation Initiative,
Department of Computer Science, School of Computing and Data Science,
The University of Hong Kong, Pokfulam Road, Hong Kong, China*

(Dated: February 6, 2025)

Extensive research has been dedicated to the asymptotic theory of quantum metrology, where the goal is to determine the ultimate precision limit of quantum channel estimation when many accesses to the channel are allowed. The ultimate limit has been well established, but in general noiseless and controllable ancilla is required for attaining it. Little is known about the metrological performance without noiseless ancilla, which is more relevant in practical circumstances. In this work, we present a novel theoretical framework to address this problem, bridging quantum metrology and the asymptotic theory of quantum channels. Leveraging this framework, we prove sufficient conditions for achieving the Heisenberg limit with repeated applications of the channel to estimate, both with and without applying interleaved unitary control operations. For the latter case, we design an algorithm to identify explicitly the control operation.

Introduction—Quantum metrology [1–3] is one of the most promising quantum technologies in and beyond the noisy intermediate-scale quantum (NISQ) era [4]. Its power has already been demonstrated in a wide range of contexts including gravitational wave detection [5, 6], quantum clocks [7, 8], and high-resolution imaging [9, 10].

The goal of quantum metrology is to boost the precision of estimating some unknown physical parameter utilizing quantum resources. In a prototypical setup, one would like to estimate a parameter θ , given N queries to an unknown quantum channel \mathcal{E}_θ in each round of the experiment. By leveraging quantum entanglement in preparing a probe state (parallel strategy) [1, 2], or coherently applying a sequence of \mathcal{E}_θ interleaved with control operations (sequential strategy) [2, 11, 12], the ultimate limit of mean squared error (MSE) $\delta\hat{\theta}^2$ is the Heisenberg limit (HL) $1/N^2$. The $1/N^2$ scaling is known to hold for unitary channel estimation [13] but is susceptible to noise [14], which sometimes results in the standard quantum limit (SQL) $1/N$, hindering the quantum scaling advantage. It is thus a desideratum to investigate under what types of noise the HL is still achievable.

Extensive research has focused on identifying the ultimate precision limit for quantum channel estimation [12, 14–22]. Both parallel and sequential strategies achieve the same optimal asymptotic scaling [22], either the HL or the SQL, depending on whether the channel to estimate satisfies the “Hamiltonian-not-in-Kraus-span” (HNKS) condition [21]. However, the attainability of the optimal precision limit, in general, assumed that one has unbounded quantum memory when $N \rightarrow \infty$. When the HL can be achieved with sequential strategies, there is no need for the unbounded memory, but noiseless ancilla and syndrome measurements are required for repeatedly applying quantum error correction (QEC) [19–21].

The requirement of noiseless ancilla, however, is a major obstacle in many real-world applications. To circumvent this issue, ancilla-free probe states have been

proposed in some metrological strategies [23, 24], which, nevertheless, either require highly entangled many-body probe states, or involve real-time syndrome measurements and delicate QEC operations that introduce additional ancilla. Such requirements are not only challenging for near-term devices [25, 26], but also impose strong demands on the programmability of quantum sensors even in the long term.

In this Letter, we establish a theoretical framework for single-parameter quantum channel estimation with ancilla-free sequential strategies and uncover a close connection between metrological limits and the spectral properties of quantum channels. In contrast to existing results that rely on QEC, we apply our framework to identify sufficient conditions for achieving the *ancilla-free HL* [27], with either control-free strategies, or identical unitary control operations that can be systematically identified by an algorithm. We summarize our main results in Table I. The strategies we consider can be implemented by the simple setup in Fig. 1, motivated by typical optical experiments, where it is favorable to apply identical unitary control operations in an optical loop [25].

TABLE I. Comparison of main results with previous works.

Scaling	Condition	Strategy
SQL [19–21]	HNKS violated	QEC, unbounded ancilla
HL [19–21]	HNKS satisfied	QEC, bounded ancilla
Ancilla-free HL	Theorem 1	Control-free
	Theorem 2 ^a	Unitary control

^a See Theorem 3 for a special case in terms of parameter estimation under Pauli noise.

Lower bound on quantum Fisher information—Given a single-parameter quantum state ρ_θ , the MSE $\delta\hat{\theta}^2 := \mathbb{E}[(\hat{\theta} - \theta)^2]$ for any unbiased estimator $\hat{\theta}$ is restricted by the quantum Cramér-Rao bound (QCRB) [28–30] $\delta\hat{\theta}^2 \geq 1/[\nu F^Q(\rho_\theta)]$, where $F^Q(\rho_\theta)$ is the quantum Fisher

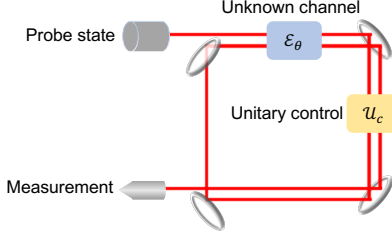


FIG. 1. Control-enhanced sequential strategy for estimating θ from N queries to \mathcal{E}_θ ($N = 2$ as an illustrated example). Trivial $\mathcal{U}_c = \mathcal{I}$ corresponds to a control-free strategy.

information (QFI) and ν is the number of times the experiment is repeated. As the bound is achievable in the limit of large ν , the QFI can be regarded as a score function for single-parameter quantum metrology, quantifying the sensitivity of ρ_θ to θ . Note that QFI is relevant for *local estimation* in the neighborhood of the true value $\theta = \theta_0$ [31]. In quantum channel estimation, we focus on the QFI of the output state ρ_θ of protocols that query the channel \mathcal{E}_θ for N times. We say the HL (SQL) is achieved if the QFI scales as N^2 (N), as $N \rightarrow \infty$.

The QFI is defined as $F^Q(\rho_\theta) := \text{Tr}(\rho_\theta L_{\rho_\theta}^2)$, where L_{ρ_θ} is the symmetric logarithmic derivative (SLD) defined through $2\dot{\rho}_\theta = \rho_\theta L_{\rho_\theta} + L_{\rho_\theta} \rho_\theta$, having denoted the derivative of X with respect to θ by \dot{X} . For a pure state $\rho_\theta = |\psi_\theta\rangle\langle\psi_\theta|$, the QFI can be computed in a simpler way:

$$F^Q(|\psi_\theta\rangle\langle\psi_\theta|) = 4 \left(\langle \dot{\psi}_\theta | \dot{\psi}_\theta \rangle - |\langle \psi_\theta | \dot{\psi}_\theta \rangle|^2 \right). \quad (1)$$

In general, however, it can be challenging to analytically evaluate the QFI of N queries to the channel \mathcal{E}_θ for large N , as computing the SLD L_{ρ_θ} requires the spectral decomposition of ρ_θ [30]. It is thus more practical to obtain a lower bound on the QFI, which already suffices to provide a guaranteed precision scaling. To this end, we employ a technique based on vectorization to derive such an efficiently computable lower bound.

We first bound the state QFI $F^Q(\rho_\theta)$ and then investigate its scaling with N . Here, it is useful to represent a quantum state ρ on d -dimensional Hilbert space \mathcal{H} as a d^2 -dimensional vector $|\rho\rangle\rangle$, where $|\rho\rangle\rangle = \sum_{ij} \langle i|\rho|j\rangle |i\rangle|j\rangle$ denotes the vectorization of ρ in the computational basis $\{|i\rangle\}_i$. Ref. [35] showed that, $F^Q(\rho_\theta)$ has a close relation to the *associated QFI*

$$\tilde{F}^Q(\tilde{\rho}_\theta) = \text{Tr}(\tilde{\rho}_\theta L_{\tilde{\rho}_\theta}^2), \quad (2)$$

where $\tilde{\rho}_\theta := |\rho_\theta\rangle\rangle\langle\langle\rho_\theta| / \text{Tr}(\rho_\theta^2)$ is the density operator of the *associated state*, and $L_{\tilde{\rho}_\theta}$ is the *associated SLD* defined by $2\dot{\tilde{\rho}}_\theta = \tilde{\rho}_\theta L_{\tilde{\rho}_\theta} + L_{\tilde{\rho}_\theta} \tilde{\rho}_\theta$. Specifically, the QFI of ρ_θ can be lower bounded by the associated QFI up to a non-vanishing multiplicative factor [35]:

$$F^Q(\rho_\theta) \geq \frac{\text{Tr}(\rho_\theta^2)}{4\lambda_{\max}(\rho_\theta)} \tilde{F}^Q(\tilde{\rho}_\theta), \quad (3)$$

where $\lambda_{\max}(\rho_\theta)$ is the largest eigenvalue of ρ_θ .

In this Letter, we focus on the scaling of the associated QFI $\tilde{F}^Q(\tilde{\rho}_\theta)$, which is easier to compute and serves as a sufficient condition for attaining the same scaling in terms of the original QFI $F^Q(\rho_\theta)$. As a starting point, we slightly generalize the result in Ref. [35] and introduce a lemma providing a closed-form formula for $\tilde{F}^Q(\tilde{\rho}_\theta)$ (see the proof in Ref. [36]).

Lemma 1. *The associated QFI of the associated state $\tilde{\rho}_\theta = |\rho_\theta\rangle\rangle\langle\langle\rho_\theta| / \text{Tr}(\rho_\theta^2)$ is given by*

$$\tilde{F}^Q(\tilde{\rho}_\theta) = 4 \left\{ \frac{\langle\langle \dot{\rho}_\theta | \dot{\rho}_\theta \rangle\rangle}{\text{Tr}(\rho_\theta^2)} - \left[\frac{\langle\langle \rho_\theta | \dot{\rho}_\theta \rangle\rangle}{\text{Tr}(\rho_\theta^2)} \right]^2 \right\}. \quad (4)$$

Note that Eq. (4) takes a simple form analogous to the pure state QFI given by Eq. (1).

Asymptotics of quantum channels—Before delving into the scaling of $\tilde{F}^Q(\tilde{\rho}_\theta)$, let us briefly recall some spectral properties of quantum channels. A quantum channel, i.e., a completely positive and trace preserving (CPTP) map, \mathcal{E}_θ , can be described by Kraus operators: $\mathcal{E}_\theta(\rho) = \sum_{i=1}^r K_i^\theta \rho K_i^{\theta\dagger}$. When treated as a superoperator, a quantum channel acting on a d -dimensional system has a *Liouville representation* [43, 44] given by a $d^2 \times d^2$ transition matrix [45]

$$T_\theta := \sum_{i=1}^r K_i^\theta \otimes K_i^{\theta*}. \quad (5)$$

Now we can express the action of the quantum channel on a state as the multiplication of a matrix by a vector, i.e., we have $|\mathcal{E}_\theta(\rho)\rangle\rangle = T_\theta |\rho\rangle\rangle$.

We focus on the spectral properties of T_θ (see Refs. [46–48] for further details). Consider the spectrum $\{\lambda_i\}_i$ of T_θ , such that $T_\theta |R_i\rangle\rangle = \lambda_i |R_i\rangle\rangle$. For clarity, we call $\{|R_i\rangle\rangle\}_i$ the *eigenvectors* and $\{R_i\}_i$ the *eigenmatrices*. All the eigenvalues satisfy $|\lambda_i| \leq 1$ (with at least one $\lambda_j = 1$ associated with the *fixed point state* ρ_*), and those satisfying $|\lambda_i| = 1$ are called *peripheral eigenvalues*, with the corresponding eigenvectors called *peripheral eigenvectors*.

We denote the set of indices of peripheral eigenvalues by \mathcal{S} . In general, T_θ is not necessarily diagonalizable, but may only admit a Jordan normal form. However, for the peripheral eigenvalues $\{\lambda_i | i \in \mathcal{S}\}$, the Jordan blocks are all one-dimensional [46, Proposition 6.2]. In the asymptotic limit of applying N quantum channels repeatedly, i.e., applying T_θ^N , only the peripheral eigenvalues and eigenvectors take effect in the output $\lim_{N \rightarrow \infty} T_\theta^N |\rho\rangle\rangle$, which could greatly facilitate our later analysis.

Achieving the HL without control—Now we first consider applying the quantum channel \mathcal{E}_θ N times sequentially without any control. The goal is thus to evaluate the QFI of $\rho_\theta = \mathcal{E}_\theta^N(\rho_0)$ for a suitable probe state ρ_0 . With the vectorization trick, we can focus on the associated QFI for $T_\theta^N |\rho_0\rangle\rangle$ to obtain a lower bound on

$F^Q[\mathcal{E}_\theta^N(\rho_0)]$. Leveraging Lemma 1, we can connect the asymptotic associated QFI to the spectral properties of T_θ as follows.

Lemma 2. Consider a quantum channel T_θ defined by Eq. (5) with peripheral eigenvalues $\{\lambda_i \mid i \in \mathcal{S}\}$ and peripheral eigenvectors $\{|R_i\rangle\rangle \mid i \in \mathcal{S}\}$. For any input state $|\rho_0\rangle\rangle = \sum_{i=1}^{d^2} a_i |R_i\rangle\rangle$ (having chosen a set of linearly independent vectors $\{|R_i\rangle\rangle\}_{i=1}^{d^2}$ that forms a Jordan basis [49]), by the repeated application of T_θ for $N \rightarrow \infty$ times, the asymptotic associated QFI of $\tilde{\rho}_\theta = |\rho_\theta\rangle\rangle\langle\langle\rho_\theta| / \text{Tr}(\rho_\theta^2)$ for $|\rho_\theta\rangle\rangle = T_\theta^N |\rho_0\rangle\rangle$ is given by

$$\lim_{N \rightarrow \infty} \frac{\tilde{F}^Q(\tilde{\rho}_\theta)}{N^2} = 4 \left[\sum_{i,j \in \mathcal{S}} \beta_{ij} \frac{\dot{\lambda}_i^* \dot{\lambda}_j}{\lambda_i^* \lambda_j} - \left(\sum_{i,j \in \mathcal{S}} \beta_{ij} \frac{\dot{\lambda}_j}{\lambda_j} \right)^2 \right], \quad (6)$$

where $\beta_{ij} = (\lambda_i^* \lambda_j)^N a_i a_j \langle\langle R_i | R_j \rangle\rangle / \text{Tr}(\rho_\theta^2)$ satisfying $\sum_{i,j \in \mathcal{S}} \beta_{ij} = 1$ and $\beta_{ji} = \beta_{ij}^*$ [50].

Lemma 2 straightforwardly yields a sufficient condition for achieving the HL without control, formulated as the existence of the nonzero derivative of a peripheral eigenvalue, as stated in Theorem 1 (see the proofs of Lemma 2 and Theorem 1 in Ref. [36]).

Theorem 1. If, at $\theta = \theta_0$, there exists some peripheral eigenvalue λ_j such that $\dot{\lambda}_j \neq 0$, then the output state QFI achieves the HL by the repeated application of T_θ without control. The input state can be taken as $\rho_0 = (1 - \alpha)I/d + \alpha\rho_* + \beta(R_j + R_j^\dagger)$, where $\alpha, \beta > 0$ are arbitrary parameters for ρ_0 to be a legitimate density matrix and R_j is the peripheral eigenmatrix associated with λ_j .

Achieving the HL with unitary control—The simple condition provided by Theorem 1 does not hold in some metrological scenarios. For instance, the HL cannot be achieved without control for estimating θ given N queries to a unitary channel $\mathcal{U}_\theta(\cdot) = U_\theta \cdot U_\theta^\dagger$, where $U_\theta = e^{-i(\cos \theta \sigma_x + \sin \theta \sigma_z)}$ [13, 51, 52]. One can check that all the peripheral eigenvalues of $U_\theta \otimes U_\theta^*$ have vanishing derivatives, as only the eigenbasis changes with θ . Nevertheless, we can apply a unitary control $U_{\theta_0}^\dagger$ following each query to U_θ to recover the HL at $\theta = \theta_0$.

It is thus natural to ask under what circumstances it is possible to apply unitary control to achieve the HL in noisy metrology, which remains largely unexplored. Based on Theorem 1, we prove a sufficient condition for achieving the HL with interleaved identical unitary control operations.

Theorem 2. Consider estimating a quantum channel T_θ defined by Eq. (5). We denote by P the projection on the subspace \mathcal{P} of eigenvectors of $T_\theta^\dagger T_\theta$ with eigenvalues 1. If at $\theta = \theta_0$, (i)

$$PT_\theta^\dagger \dot{T}_\theta P \neq 0 \quad (\text{non-vanishing signal}) \quad (7)$$

and (ii) there exists a unitary U_c such that for some eigenmatrix R_0 of $PT_\theta^\dagger \dot{T}_\theta P$ associated with a nonzero eigenvalue

$$U_c^\dagger R_0 U_c = \sum_k K_k^\theta R_0 K_k^{\theta\dagger} \quad (\text{partially reversible}) \quad (8)$$

then the output state QFI achieves the HL by applying the same unitary control U_c following each channel T_θ .

The proof is provided in Ref. [36]. The two conditions in Theorem 2 have intuitive interpretations. The first condition indicates that the signal operator $T_\theta^\dagger \dot{T}_\theta$ has a nontrivial effect on the subspace \mathcal{P} , and the second condition ensures that the effective action of the quantum channel on R_0 is reversible, simulated by a unitary operation. By appending the unitary control U_c to T_θ , the strategy reduces to the repeated application of $(U_c \otimes U_c^*)T_\theta$ and therefore Theorem 1 is applicable.

Sketch of an algorithm for unitary control—We further design a numerical algorithm (see Algorithm 1 in Ref. [36]) that can successfully identify a unitary control operation U_c if and only if Eq. (8) can be satisfied. Note that, except for the trivial case where R_0 and R_0^\dagger are associated with the same eigenvalue of $PT_\theta^\dagger \dot{T}_\theta P$ (such that R_0 can be chosen as a Hermitian matrix and finding U_c is trivial), Eq. (8) can be reformulated as

$$U_c^\dagger R_i U_c = \sum_k K_k^{\theta_0} R_i K_k^{\theta_0\dagger}, \quad \forall i = 1, 2, \quad (9)$$

where $R_1 = R_0 + R_0^\dagger$ and $R_2 = i(R_0 - R_0^\dagger)$ are two Hermitian matrices. The key idea behind the algorithm is using the principal angles [53–55] to characterize the relation between subspaces. For two arbitrary subspaces F and G associated with projections Π_F and Π_G on the subspaces, the principal angles can be determined by performing the singular value decomposition (SVD) of $\Pi_F \Pi_G$ (i.e., the principal angles are arccosine values of the singular values). The geometrical relation between two subspaces can then be fully characterized by the relation between a set of subspaces of lower dimensions. By iterative reduction of the dimensions of subspaces, at last, the reduced subspaces either are mutually orthogonal to each other or share equal dimensions and degenerate principal angles. It is thus possible to choose a set of canonical orthonormal vectors for each subspace, and the inner products between these vectors are uniquely determined. If U_c satisfying Eq. (8) exists, all the inner products are preserved by the action of T_θ , so we can choose a unitary transformation to simulate the effect. We leave the detailed proof of the validity of the algorithm in Ref. [36].

Achieving the HL under Pauli noise—For parameter estimation under Pauli noise, a widely considered scenario in quantum metrology [12, 14, 16–22, 56–59], our framework yields a convenient criterion for achieving the ancilla-free HL.

Consider estimating an n -qubit channel T_θ defined by Eq. (5), where

$$K_i^\theta = \sqrt{p_i} V_\theta P_i U_\theta, \quad i = 1, \dots, r, \quad (10)$$

$\sum_{i=1}^r p_i = 1$ with each $p_i > 0$, and $\{P_i\}_i$ are (n -qubit) Pauli operators (having included the identity operator I in $\{P_i\}_i$ [60]). U_θ and V_θ are both unitary operators encoding the parameter. The generators associated with the signal before and after the noise are $H^{(U)} := iU_\theta^\dagger \dot{U}_\theta$ and $H^{(V)} := iV_\theta^\dagger \dot{V}_\theta$, and we define $H_{\text{tot}} := H^{(U)} + H^{(V)}$. We decompose $H_{\text{tot}} = \sum_k \alpha_k Q_k$, where $\{Q_k\}_k$ are (n -qubit) Pauli operators (including the identity) and each $\alpha_k \neq 0$ (see the proof in Ref. [36]).

Theorem 3. *For Kraus operators given by Eq. (10), if, at $\theta = \theta_0$, there exists some Q_k such that (i) [61]*

$$Q_k \notin \text{Span}\{\{P_1, P_2, \dots, P_r\}\}, \quad (11)$$

and (ii)

$$[Q_k, P_i] = 0, \quad \forall i = 1, \dots, r, \quad (12)$$

then the output state QFI achieves the HL by applying the same unitary control $U_c = U_{\theta_0}^\dagger V_{\theta_0}^\dagger$ following each channel T_θ .

We remark that Eq. (11) in Theorem 3 can be reformulated as $H_{\text{tot}} \notin \text{Span}\{\{P_1, P_2, \dots, P_r\}\}$, resembling but stricter than the HNKS condition: $H := i\sum_{k=1}^r K_k^{\theta\dagger} \dot{K}_k^\theta \notin \text{Span}\{K_i^{\theta\dagger} K_j^\theta, \forall i, j\}$ [21]. To see this, we assume that $U_{\theta_0} = V_{\theta_0} = I$ for simplicity; otherwise, appropriate unitary control can be applied to counteract the effects of U_θ and V_θ . At $\theta = \theta_0$, the ‘‘Hamiltonian’’ $H = i\sum_{k=1}^r K_k^{\theta\dagger} \dot{K}_k^\theta = H^{(U)} + \sum_{i=1}^r p_i P_i H^{(V)} P_i$, and the ‘‘Kraus span’’ becomes a linear span of Pauli operators $\text{Span}\{P_i P_j, \forall i, j\}$. Noting that, by Eq. (12) of Theorem 3, H_{tot} contains a Pauli term Q_k that commutes with all P_i for $i = 1, \dots, r$, Eq. (11) is equivalent to $H \notin \text{Span}\{\{P_1, P_2, \dots, P_r\}\}$. This indicates that the Hamiltonian lies outside not only the ‘‘Kraus span’’, but also the linear span of the group elements generated by the Pauli noise operators. While it was previously known that ancilla-assisted QEC enables achieving the HL when the HNKS condition is satisfied, we discover how this condition could be adapted such that there is no need to construct QEC codes and only unitary control operation is required.

A working example—Consider estimating a two-qubit noisy channel T_θ defined by Eq. (5), characterized by the Kraus operators $K_i^\theta = K_i^{(\text{noise})} U_t(\theta)$, where $U_t(\theta) = e^{-itH_0(\theta)}$ for the evolution time t , and the parameter θ of interest is the coupling strength in a Heisenberg model Hamiltonian

$$H_0(\theta) = \sigma_z \otimes I + I \otimes \sigma_z + \theta H_J. \quad (13)$$

for $H_J = \sigma_x \otimes \sigma_x + \sigma_y \otimes \sigma_y + \sigma_z \otimes \sigma_z$. The Pauli noise is described by

$$\begin{aligned} K_1^{(\text{noise})} &= \sqrt{1 - p_1 - p_2} I, \\ K_2^{(\text{noise})} &= \sqrt{p_1} \sigma_x \otimes \sigma_x, \\ K_3^{(\text{noise})} &= \sqrt{p_2} \sigma_x \otimes \sigma_y. \end{aligned} \quad (14)$$

Note that not all $\{K_i^{\theta\dagger} K_j^\theta\}$ commute with each other, which goes beyond the requirement of the ancilla-free QEC code protocol in Ref. [23]. It is also impossible to find a codespace stabilized by the noise as in Ref. [62]. Nevertheless, we can easily check that for this noise model the ancilla-free HL is achievable according to Theorem 3 [63].

We remark that it is unnecessary to know that the channel to estimate is in the form of Pauli noise *a priori*. To apply Theorem 2 and the algorithm for identifying the unitary control, it suffices to have the knowledge about such a ‘‘tomographic’’ description of its Liouville representation T_θ in the neighborhood of the true value θ_0 , bypassing the need to determine the type of the channel and making it more convenient for dealing with the experimental data.

Here for simplicity of presentation, we assume that we know the forms of unitary $U_t(\theta)$ and the noise $\{K_i^{(\text{noise})}\}$ respectively. Note that $T_\theta^\dagger T_\theta$ has 4 eigenvalues of 1 with eigenvectors in the subspace \mathcal{P} (associated with the projection P on it) and

$$P T_\theta^\dagger \dot{T}_\theta P = -it P T_\theta^\dagger T_\theta [H_J \otimes I - I \otimes H_J^T] P \quad (15)$$

has 2 nonzero eigenvalues, with mutually orthogonal eigenmatrices (up to multiplicative factors)

$$\begin{aligned} R_1 &= U_t(\theta)^\dagger (|01\rangle\langle 11| + |10\rangle\langle 00|) U_t(\theta), \\ R_2 &= R_1^\dagger = U_t(\theta)^\dagger (|00\rangle\langle 10| + |11\rangle\langle 01|) U_t(\theta). \end{aligned} \quad (16)$$

We can choose the unitary control

$$U_c = U_t(\theta_0)^\dagger, \quad (17)$$

and take an input state, for example,

$$\rho_0 = \frac{I}{2} \otimes \frac{I}{2} + \alpha(R_1 + R_1^\dagger) = U_t(\theta_0)^\dagger \left[\left(\frac{I}{2} + \alpha \sigma_x \right) \otimes \frac{I}{2} \right] U_t(\theta_0) \quad (18)$$

for some $0 < \alpha < 1/2$ [64], and incorporate unitary control $U_c = U_t(\theta_0)^\dagger$ after each application of T_θ . Note that if only the form of T_θ (instead of separating the unitary evolution and noise) is known, we can apply our algorithm to T_θ to find a numerical solution for U_c .

Remarkably, in this case, preparing the input state Eq. (18) is fully robust to any local state preparation error on the second qubit, i.e., the second qubit can be arbitrarily initialized. The reason is that the regulated channel $(U_c \otimes U_c^*) T_\theta$ is unitarily diagonalizable

at $\theta = \theta_0$. For an arbitrary state of the second qubit $\sigma = \frac{1}{2}(I + r_x\sigma_x + r_y\sigma_y + r_z\sigma_z)$ with $r_x^2 + r_y^2 + r_z^2 = 1$, all the contributions from $\sigma_x, \sigma_y, \sigma_z$ vanish in the asymptotic limit, as they are orthogonal to the peripheral eigenspace. Therefore, the choice of σ has no detrimental effect on achieving the guaranteed HL.

In the End Matter, we conduct additional numerical analysis to assess the error robustness of the state preparation and measurement (SPAM) as well as control in our strategy. The sequential nature of our approach is particularly well-suited for addressing SPAM errors.

It is worth noting that the control is essential for achieving the HL here. Without the control U_c, T_θ generically has only one fixed point state (the maximally mixed state) on the peripheral eigenspaces, so no information can be retrieved after $N \rightarrow \infty$ applications in a control-free strategy.

This informative example reveals three key distinctions between our approach and QEC: *i*) We provide an algorithmic routine to find the probe state and identical unitary control for achieving the ancilla-free HL in an experiment-friendly scenario, while such a routine is lacking for constructing ancilla-free QEC codes for metrology. *ii*) We do not use QEC recovery operations, which may require additional ancilla. *iii*) The probe state by our approach does not necessarily lie in a QEC codespace that satisfies the Knill-Laflamme condition [69]. Overall, our formalism works in a more resource-deficient scenario, which can be of practical interest.

Discussion—We establish a systematic formalism for ancilla-free quantum channel estimation. By vectorizing the quantum state and investigating the spectral properties of channels, we derive useful formulas for the QFI with ancilla-free sequential strategies, and identify sufficient conditions for achieving the HL, in both control-free and unitary-control-enhanced scenarios. This formalism is also applicable while allowing bounded ancilla, as the problem reduces to estimation of $\mathcal{E}_\theta \otimes \mathcal{N}_A$, where \mathcal{N}_A is the noise channel acting on the ancilla.

Our results have other surprising implications not covered in the main text. In Ref. [36] we identify examples demonstrating that it is sometimes possible to achieve the HL even when the conventional HNKS condition is ill-defined, or in the absence of decoherence-free subspace (DFS) [70].

Our approach is less resource demanding compared to the conventional QEC approach and well-suited for experimental design. Compared with our previous works [71–73], the obtained protocol is not strictly optimal but has a performance guarantee of the precision scaling. The complexity of the algorithm is much lower and does not grow with N . The simple setup allows the circuit to be looped many times, thus facilitating experimental demonstration of quantum metrology for large N .

A very recent work [74] proved that the HL is unattainable with unitary control for single-qubit noisy channel

estimation when the noise strength is nonvanishing. Interestingly, our work shows that this conclusion does not extend to higher dimensions.

Acknowledgments—This work is supported by the National Natural Science Foundation of China via Excellent Young Scientists Fund (Hong Kong and Macau) Project 12322516, Ministry of Science and Technology, China (MOST2030) with Grant No. 2023200300600, Guangdong Provincial Quantum Science Strategic Initiative (GDZX2303007 and GDZX2203001), and the Hong Kong Research Grant Council (RGC) through the Early Career Scheme (ECS) grant 27310822 and the General Research Fund (GRF) grant 17303923.

END MATTER ON ROBUSTNESS AGAINST PROTOCOL IMPERFECTIONS

Here we provide more analysis for the example presented in the main text, discussing the robustness of our approach with respect to the SPAM and control errors. Notably, the robustness against SPAM errors arises from the sequential nature of our protocol and is a general feature, not limited to the specific example discussed. More precisely, the probe state given by Theorem 1 provides the flexibility to choose parameters α and β , making it robust to state preparation error. Similar arguments hold for robustness against measurement error.

We model the SPAM error p_{SPAM} as single-qubit depolarizing noise, described by the channel $\mathcal{N}^{(\text{dep})}(\rho) = (1 - p_{\text{SPAM}})\rho + (p_{\text{SPAM}}/2)I$. Specifically, in the two-qubit example $\mathcal{N}^{(\text{dep})} \otimes \mathcal{N}^{(\text{dep})}$ occurs at both the state preparation and measurement stages.

The control error is modeled as a classical Gaussian fluctuation in the control Hamiltonian, i.e., at each intervention step the actual control is $U_c = e^{-itH_c}$, where $H_c = -BH_0(\theta_0)$ and B is a random variable drawn from the normal distribution with mean $\mu = 1.0$ and variance $\sigma_{\text{control}}^2$. We assume that B is independent and identically distributed (i.i.d.) across different control steps.

We plot the normalized output QFI $F^Q(\rho_\theta)/N$ versus the number of queries N in Fig. 2. We take $\theta_0 = 1.0$, $t = 1.0$, and $p_1 = p_2 = 0.1$. Ideally without SPAM and control errors, we prepare the input state ρ_0 given by Eq. (18) for $\alpha = 0.495$ and choose the unitary control U_c given by Eq. (17), which yields the HL as shown by the solid gray line. We also verify that in the ideal case the input state of the second qubit can be arbitrarily chosen without affecting the QFI, as predicted by the theory.

In many typical experiments, the readout noise is dominant compared to gate noise [75–78]. We find that the SPAM errors are not fatal for achieving the HL, indicated by dashed ($p_{\text{SPAM}} = 0.01$) and dotted ($p_{\text{SPAM}} = 0.1$) gray lines [79]. This can be expected, since our sequential strategy repeatedly amplifies the signal and the SPAM noise only has a constant effect in the asymptotic limit.

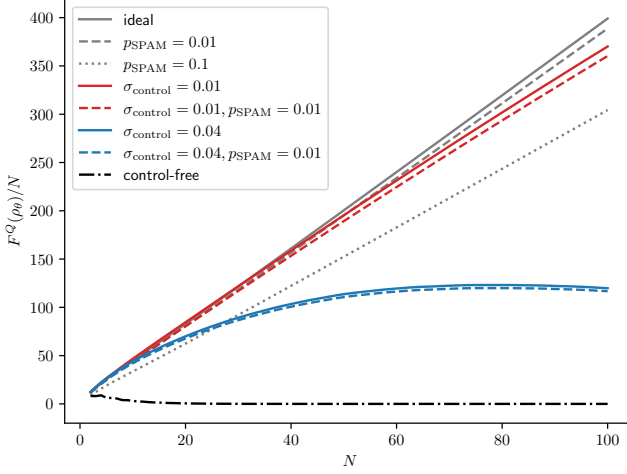


FIG. 2. The normalized output QFI $F^Q(\rho_\theta)/N$ versus the number of queries N . The (expectation value of the) QFI is computed over 1000 trials with random control errors. The gray lines represent different SPAM error rates ($p_{\text{SPAM}} = 0, 0.01, 0.1$) under ideal control ($\sigma_{\text{control}} = 0$). The red ($\sigma_{\text{control}} = 0.01$) and blue ($\sigma_{\text{control}} = 0.04$) lines show how the HL deviates as control error increases, with dashed lines corresponding to the presence of SPAM errors and solid lines indicating the absence of SPAM errors. The solid black line represents the performance of a control-free strategy.

Control errors are harder to tackle since they accumulate as N grows. Nevertheless, when the classical error in control is small ($\sigma_{\text{control}} = 0.01$), we can still observe a QFI scaling close to the HL. The deviation from the HL becomes more obvious for larger fluctuations ($\sigma_{\text{control}} = 0.04$).

As a benchmark, the dash-dotted black line depicts the performance of a control-free strategy in the ideal case without SPAM and control errors. The QFI vanishes for large N , as T_{θ_0} is a mixing channel, transforming a generic input state into the fixed point state.

* qslu@cs.hku.hk

† yuxiang@cs.hku.hk

- [1] V. Giovannetti, S. Lloyd, and L. Maccone, Quantum-enhanced measurements: Beating the standard quantum limit, *Science* **306**, 1330 (2004).
- [2] V. Giovannetti, S. Lloyd, and L. Maccone, Quantum Metrology, *Phys. Rev. Lett.* **96**, 010401 (2006).
- [3] C. L. Degen, F. Reinhard, and P. Cappellaro, Quantum sensing, *Rev. Mod. Phys.* **89**, 035002 (2017).
- [4] J. Preskill, Quantum Computing in the NISQ era and beyond, *Quantum* **2**, 79 (2018).
- [5] R. Schnabel, N. Mavalvala, D. E. McClelland, and P. K. Lam, Quantum metrology for gravitational wave astronomy, *Nat. Commun.* **1**, 121 (2010).
- [6] M. Tse *et al.*, Quantum-enhanced advanced ligo detectors in the era of gravitational-wave astronomy, *Phys. Rev. Lett.* **123**, 231107 (2019).

- [7] V. Bužek, R. Derka, and S. Massar, Optimal Quantum Clocks, *Phys. Rev. Lett.* **82**, 2207 (1999).
- [8] E. Pedrozo-Peñafiel, S. Colombo, C. Shu, A. F. Adiyatullin, Z. Li, E. Mendez, B. Braverman, A. Kawasaki, D. Akamatsu, Y. Xiao, and V. Vuletić, Entanglement on an optical atomic-clock transition, *Nature* **588**, 414 (2020).
- [9] G. Brida, M. Genovese, and I. Ruo Berchera, Experimental realization of sub-shot-noise quantum imaging, *Nat. Photonics* **4**, 227 (2010).
- [10] D. Le Sage, K. Arai, D. R. Glenn, S. J. DeVience, L. M. Pham, L. Rahn-Lee, M. D. Lukin, A. Yacoby, A. Komeili, and R. L. Walsworth, Optical magnetic imaging of living cells, *Nature* **496**, 486 (2013).
- [11] W. van Dam, G. M. D'Ariano, A. Ekert, C. Macchiavello, and M. Mosca, Optimal quantum circuits for general phase estimation, *Phys. Rev. Lett.* **98**, 090501 (2007).
- [12] R. Demkowicz-Dobrzański and L. Maccone, Using entanglement against noise in quantum metrology, *Phys. Rev. Lett.* **113**, 250801 (2014).
- [13] H. Yuan and C.-H. F. Fung, Optimal feedback scheme and universal time scaling for hamiltonian parameter estimation, *Phys. Rev. Lett.* **115**, 110401 (2015).
- [14] R. Demkowicz-Dobrzański, J. Kołodyński, and M. Guță, The elusive heisenberg limit in quantum-enhanced metrology, *Nat. Commun.* **3**, 1063 (2012).
- [15] A. Fujiwara and H. Imai, A fibre bundle over manifolds of quantum channels and its application to quantum statistics, *J. Phys. A* **41**, 255304 (2008).
- [16] B. M. Escher, R. L. de Matos Filho, and L. Davidovich, General framework for estimating the ultimate precision limit in noisy quantum-enhanced metrology, *Nat. Phys.* **7**, 406 (2011).
- [17] J. Kołodyński and R. Demkowicz-Dobrzański, Efficient tools for quantum metrology with uncorrelated noise, *New J. Phys.* **15**, 073043 (2013).
- [18] P. Sekatski, M. Skotiniotis, J. Kołodyński, and W. Dür, Quantum metrology with full and fast quantum control, *Quantum* **1**, 27 (2017).
- [19] R. Demkowicz-Dobrzański, J. Czajkowski, and P. Sekatski, Adaptive Quantum Metrology under General Markovian Noise, *Phys. Rev. X* **7**, 041009 (2017).
- [20] S. Zhou, M. Zhang, J. Preskill, and L. Jiang, Achieving the heisenberg limit in quantum metrology using quantum error correction, *Nat. Commun.* **9**, 78 (2018).
- [21] S. Zhou and L. Jiang, Asymptotic theory of quantum channel estimation, *PRX Quantum* **2**, 010343 (2021).
- [22] S. Kurdzialek, W. Górecki, F. Albarelli, and R. Demkowicz-Dobrzański, Using adaptiveness and causal superpositions against noise in quantum metrology, *Phys. Rev. Lett.* **131**, 090801 (2023).
- [23] D. Layden, S. Zhou, P. Cappellaro, and L. Jiang, Ancilla-free quantum error correction codes for quantum metrology, *Phys. Rev. Lett.* **122**, 040502 (2019).
- [24] S. Zhou, A. G. Manes, and L. Jiang, Achieving metrological limits using ancilla-free quantum error-correcting codes, *Phys. Rev. A* **109**, 042406 (2024).
- [25] Z. Hou, R.-J. Wang, J.-F. Tang, H. Yuan, G.-Y. Xiang, C.-F. Li, and G.-C. Guo, Control-Enhanced Sequential Scheme for General Quantum Parameter Estimation at the Heisenberg Limit, *Phys. Rev. Lett.* **123**, 040501 (2019).

- [26] Z. Hou, Y. Jin, H. Chen, J.-F. Tang, C.-J. Huang, H. Yuan, G.-Y. Xiang, C.-F. Li, and G.-C. Guo, “superheisenberg” and heisenberg scalings achieved simultaneously in the estimation of a rotating field, *Phys. Rev. Lett.* **126**, 070503 (2021).
- [27] In this work we only care about the precision scaling $1/N^2$, regardless of the coefficient.
- [28] C. W. Helstrom, *Quantum Detection and Estimation Theory* (Academic Press, New York, 1976).
- [29] A. S. Holevo, *Probabilistic and Statistical Aspects of Quantum Theory* (North-Holland Publishing Company, Amsterdam, 1982).
- [30] S. L. Braunstein and C. M. Caves, Statistical distance and the geometry of quantum states, *Phys. Rev. Lett.* **72**, 3439 (1994).
- [31] Certainly, the true value θ_0 should only be roughly known before the experiment. In practice, one can adaptively update the metrological strategy based on the previous estimate $\hat{\theta}$ during the experiment [32–34].
- [32] O. E. Barndorff-Nielsen and R. D. Gill, Fisher information in quantum statistics, *J. Phys. A* **33**, 4481 (2000).
- [33] M. Hayashi, Comparison between the cramer-rao and the mini-max approaches in quantum channel estimation, *Commun. Math. Phys.* **304**, 689 (2011).
- [34] Y. Yang, G. Chiribella, and M. Hayashi, Attaining the ultimate precision limit in quantum state estimation, *Commun. Math. Phys.* **368**, 223 (2019).
- [35] S. Alipour, M. Mehboudi, and A. T. Rezakhani, Quantum metrology in open systems: Dissipative cramer-rao bound, *Phys. Rev. Lett.* **112**, 120405 (2014).
- [36] See Supplemental Material, which includes Ref. [37–42], for preliminaries, proofs and additional examples.
- [37] D. E. Evans and R. Höegh-Krohn, Spectral properties of positive maps on c^* -algebras, *J. Lond. Math. Soc.* **s2-17**, 345 (1978).
- [38] V. V. Albert, Asymptotics of quantum channels: conserved quantities, an adiabatic limit, and matrix product states, *Quantum* **3**, 151 (2019).
- [39] C. Neill, P. Roushan, M. Fang, Y. Chen, M. Kolodrubetz, Z. Chen, A. Megrant, R. Barends, B. Campbell, B. Chiaro, A. Dunsworth, E. Jeffrey, J. Kelly, J. Mutus, P. J. J. O’Malley, C. Quintana, D. Sank, A. Vainsencher, J. Wenner, T. C. White, A. Polkovnikov, and J. M. Martinis, Ergodic dynamics and thermalization in an isolated quantum system, *Nat. Phys.* **12**, 1037 (2016).
- [40] R. Movassagh and J. Schenker, Theory of ergodic quantum processes, *Phys. Rev. X* **11**, 041001 (2021).
- [41] https://github.com/qiushi-liu/unitary_control_for_metrology.
- [42] J. C. Gower and G. B. Dijkstra, *Procrustes Problems* (Oxford University Press, New York, 2004).
- [43] A. Gilchrist, D. R. Terno, and C. J. Wood, Vectorization of quantum operations and its use (2011), [arXiv:0911.2539](https://arxiv.org/abs/0911.2539).
- [44] C. J. Wood, J. D. Biamonte, and D. G. Cory, Tensor networks and graphical calculus for open quantum systems, *Quantum Inf. Comput.* **15**, 759–811 (2015).
- [45] Here we only consider quantum channels with equal input and output spaces.
- [46] M. M. Wolf, Quantum channels & operations: Guided tour (2012), <https://mediatum.ub.tum.de/doc/1701036/document.pdf>.
- [47] D. Burgarth, G. Chiribella, V. Giovannetti, P. Perinotti, and K. Yuasa, Ergodic and mixing quantum channels in finite dimensions, *New J. Phys.* **15**, 073045 (2013).
- [48] J. Watrous, *The Theory of Quantum Information* (Cambridge University Press, Cambridge, England, 2018).
- [49] The choices of $|R_i\rangle$ coincide with the peripheral eigenvectors of T_θ when $i \in S$.
- [50] We assume that $\lambda_i, |R_i\rangle, a_i$ are all continuously differentiable with respect to θ .
- [51] S. Pang and T. A. Brun, Quantum metrology for a general hamiltonian parameter, *Phys. Rev. A* **90**, 022117 (2014).
- [52] J. Liu, X.-X. Jing, and X. Wang, Quantum metrology with unitary parametrization processes, *Sci. Rep.* **5**, 8565 (2015).
- [53] C. Jordan, Essai sur la géométrie à n dimensions, *Bull. Soc. Math. France* **3**, 103 (1875).
- [54] Å. Björck and G. H. Golub, Numerical methods for computing angles between linear subspaces, *Math. Comput.* **27**, 579 (1973), full publication date: Jul., 1973.
- [55] A. Galántai and C. J. Hegedűs, Jordan’s principal angles in complex vector spaces, *Numer. Linear Algebra Appl.* **13**, 589 (2006).
- [56] G. Arrad, Y. Vinkler, D. Aharonov, and A. Retzker, Increasing sensing resolution with error correction, *Phys. Rev. Lett.* **112**, 150801 (2014).
- [57] E. M. Kessler, I. Lovchinsky, A. O. Sushkov, and M. D. Lukin, Quantum Error Correction for Metrology, *Phys. Rev. Lett.* **112**, 150802 (2014).
- [58] R. Ozeri, Heisenberg limited metrology using quantum error-correction codes (2013), [arXiv:1310.3432](https://arxiv.org/abs/1310.3432).
- [59] W. Dür, M. Skotiniotis, F. Fröwis, and B. Kraus, Improved Quantum Metrology Using Quantum Error Correction, *Phys. Rev. Lett.* **112**, 080801 (2014).
- [60] We assume that the Kraus operators of the Pauli noise channel contain a term proportional to identity, which is a common case in practice.
- [61] $\langle a, b, \dots, c \rangle$ denotes the group generated by a, b, \dots, c . Span denotes the linear span of the set of group elements.
- [62] F. R. F. Pereira, S. Mancini, and G. G. La Guardia, Stabilizer codes for open quantum systems, *Sci. Rep.* **13**, 10540 (2023).
- [63] Note that we can choose $Q_k = \sigma_z \otimes \sigma_z$ in $H_{\text{tot}} = \sigma_x \otimes \sigma_x + \sigma_y \otimes \sigma_y + \sigma_z \otimes \sigma_z$, and the linear span of group elements generated by the Pauli noise operators is $\text{Span}\{I, \sigma_x \otimes \sigma_x, \sigma_x \otimes \sigma_y, I \otimes \sigma_z\}$.
- [64] Here we do not choose $\alpha = 1/2$ corresponding to a pure state, such that the rank of the output state is independent of θ at $\theta = \theta_0$, to avoid the possible discontinuity issue of the QFI at the rank changing point. See Refs. [65–68] for more discussions.
- [65] D. Šafránek, Discontinuities of the quantum fisher information and the bures metric, *Phys. Rev. A* **95**, 052320 (2017).
- [66] L. Seveso, F. Albarelli, M. G. Genoni, and M. G. A. Paris, On the discontinuity of the quantum fisher information for quantum statistical models with parameter dependent rank, *J. Phys. A* **53**, 02LT01 (2019).
- [67] S. Zhou and L. Jiang, An exact correspondence between the quantum fisher information and the bures metric (2019), [arXiv:1910.08473](https://arxiv.org/abs/1910.08473).
- [68] Y. Ye and X.-M. Lu, Quantum cramer-rao bound for quantum statistical models with parameter-dependent rank, *Phys. Rev. A* **106**, 022429 (2022).
- [69] E. Knill and R. Laflamme, Theory of quantum error-correcting codes, *Phys. Rev. A* **55**, 900 (1997).

- [70] D. A. Lidar, I. L. Chuang, and K. B. Whaley, Decoherence-free subspaces for quantum computation, *Phys. Rev. Lett.* **81**, 2594 (1998).
- [71] A. Altherr and Y. Yang, Quantum metrology for non-markovian processes, *Phys. Rev. Lett.* **127**, 060501 (2021).
- [72] Q. Liu, Z. Hu, H. Yuan, and Y. Yang, Optimal strategies of quantum metrology with a strict hierarchy, *Phys. Rev. Lett.* **130**, 070803 (2023).
- [73] Q. Liu, Z. Hu, H. Yuan, and Y. Yang, Fully-optimized quantum metrology: Framework, tools, and applications, *Adv. Quantum Technol.* **7**, 2400094 (2024).
- [74] S. Zhou, Limits of noisy quantum metrology with restricted quantum controls, *Phys. Rev. Lett.* **133**, 170801 (2024).
- [75] F. Arute *et al.*, Quantum supremacy using a programmable superconducting processor, *Nature* **574**, 505 (2019).
- [76] S. A. Moses *et al.*, A race-track trapped-ion quantum processor, *Phys. Rev. X* **13**, 041052 (2023).
- [77] D. Bluvstein, S. J. Evered, A. A. Geim, S. H. Li, H. Zhou, T. Manovitz, S. Ebadi, M. Cain, M. Kalinowski, D. Hangleiter, J. P. Bonilla Ataides, N. Maskara, I. Cong, X. Gao, P. Sales Rodriguez, T. Karolyshyn, G. Semeghini, M. J. Gullans, M. Greiner, V. Vuletić, and M. D. Lukin, Logical quantum processor based on reconfigurable atom arrays, *Nature* **626**, 58 (2024).
- [78] For the device specifications of IBM Quantum Processing Units, refer to <https://quantum.ibm.com/services/resources>.
- [79] The chosen values of p_{SPAM} are common in current quantum devices [78].

SUPPLEMENTAL MATERIAL

Section A introduces the preliminaries on the vectorization technique and the spectral properties of quantum channels, which turn out to be useful throughout the proof. Section B contains the proof of Lemma 1 for a closed-form expression of the associated QFI. Section C contains the proof of Lemma 2 for connecting the output associated QFI to the spectral properties of a quantum channel in the asymptotic limit. In Sections D and E we prove the conditions for achieving the ancilla-free HL without control and with unitary control, respectively summarized in Theorems 1 and 2. A detailed description and proof of the algorithm for unitary control is given in Section F. In Section G we prove conditions for achieving the HL in parameter estimation under Pauli noise. Finally, Section H presents supplemental examples demonstrating the singularity of HNKs condition and the attainability of the HL in absence of DFS.

Appendix A: Preliminaries

1. Vectorization

For a linear operator A on a d -dimensional Hilbert space \mathcal{H} , we denote its vectorization as

$$|A\rangle\rangle := \sum_{ij} \langle i|A|j\rangle |i\rangle |j\rangle, \quad (\text{A1})$$

where $\{|i\rangle \in \mathcal{H}\}_i$ and $\{|j\rangle \in \mathcal{H}\}_j$ represent the computational basis. It is easy to check that

$$|A\rangle\rangle = (A \otimes I) |\Phi\rangle \quad (\text{A2})$$

for the (unnormalized) maximally entangled state $|\Phi\rangle = \sum_i |i\rangle |i\rangle$. We denote the adjoint of $|A\rangle\rangle$ as $\langle\langle A| := |A\rangle\rangle^\dagger$ and the complex conjugate of $|A\rangle\rangle$ as $|A^*\rangle\rangle$.

We present several properties that are straightforward to obtain. Given an operator $M = \sum_k |u_k\rangle\langle v_k|$ for all $|u_k\rangle, |v_k\rangle \in \mathcal{H}$, we have

$$|M\rangle\rangle = \sum_k |u_k\rangle \otimes |v_k^*\rangle. \quad (\text{A3})$$

The Hilbert-Schmidt inner product between two operators A and B is preserved by vectorization, i.e.,

$$\text{Tr}(A^\dagger B) = \langle\langle A|B\rangle\rangle. \quad (\text{A4})$$

A particularly useful identity we will use throughout the proofs is

$$|ABC\rangle\rangle = (A \otimes C^T) |B\rangle\rangle, \quad (\text{A5})$$

for any operators A , B and C .

Interested readers can refer to Refs. [35, 48] for more details pertaining to the operator-vector correspondence.

2. Spectral properties of quantum channels

By vectorizing the density operator ρ of a d -dimensional quantum state into $|\rho\rangle\rangle$, the action of a quantum channel $\mathcal{E}(\rho) = \sum_{i=1}^r K_i \rho K_i^\dagger$ can be expressed as

$$|\mathcal{E}(\rho)\rangle\rangle = \sum_{i=1}^r (K_i \otimes K_i^*) |\rho\rangle\rangle, \quad (\text{A6})$$

having used the identity Eq. (A5). Hence, we can define a $d^2 \times d^2$ transition matrix

$$T := \sum_{i=1}^r K_i \otimes K_i^*. \quad (\text{A7})$$

to represent the quantum channel, and its action is given by $|\mathcal{E}(\rho)\rangle\rangle = T|\rho\rangle\rangle$.

As T is associated with a CPTP map, it has many useful properties [46–48], and we will review some relevant ones here. Specifically, we consider quantum channels with equal input and output spaces, and assign a spectrum $\{\lambda_i\}_i$ to T such that $T|R_i\rangle\rangle = \lambda_i|R_i\rangle\rangle$. For clarity we call $\{|R_i\rangle\rangle\}_i$ the eigenvectors and $\{|R_i\rangle\rangle\}_i$ the eigenmatrices. Note that T is not necessarily diagonalizable and admits up to d^2 eigenvalues.

1. The eigenvalues of T are either real or come in complex conjugate pairs, i.e., if λ_i is an eigenvalue of T , then λ_i^* is also an eigenvalue of T . In fact, we have $T|R_i\rangle\rangle = \lambda_i|R_i\rangle\rangle$ and $T|R_i^\dagger\rangle\rangle = \lambda_i^*|R_i^\dagger\rangle\rangle$. If λ_i is real, we can take R_i to be Hermitian.
2. All the eigenvalues of T satisfy $|\lambda_i| \leq 1$, confined in the unit circle on the complex plane. Those eigenvalues satisfying $|\lambda_i| = 1$ are called *peripheral eigenvalues*. We denote the set of indices of peripheral eigenvalues by $S := \{i \mid |\lambda_i| = 1\}$.
3. All Jordan blocks for peripheral eigenvalues are one-dimensional [46, Proposition 6.2].
4. Any quantum channel must have at least one *fixed point state*, i.e., there exists a density operator ρ_* such that $T|\rho_*\rangle\rangle = |\rho_*\rangle\rangle$.
5. A quantum channel is said to be *ergodic* if there exists a unique fixed point state ρ_* . This requirement is strong enough to guarantee that T has only one *fixed point*, i.e., eigenvector associated with unit eigenvalue $\lambda = 1$.
6. A quantum channel \mathcal{E} is said to be *mixing* if there exists a fixed point state ρ_* such that

$$\lim_{N \rightarrow \infty} \|\mathcal{E}^N(\rho) - \rho_*\| = 0, \quad \forall \rho \text{ as a density operator.} \quad (\text{A8})$$

A channel is mixing iff it is ergodic and does not have any other peripheral eigenvalue except for $\lambda = 1$.

7. As T is a trace-preserving map, we have $\text{Tr } R_j = 0$ if $\lambda_j \neq 1$.

Remark—Our framework establishes a close relation between the metrological limit and the spectral properties of quantum channels. It thus provides a new perspective on quantum metrology drawn from the asymptotic theory of quantum channels, where researchers have shown great interest in quantum ergodicity and mixing [37–40, 46, 47]. We expect that our results may also have applications in these areas beyond quantum metrology.

Appendix B: Proof of Lemma 1

Proof. By noting that $\tilde{\rho}_\theta^2 = \tilde{\rho}_\theta$, we can take the SLD $L_{\tilde{\rho}_\theta} = 2\dot{\tilde{\rho}}_\theta$. It follows that

$$\begin{aligned} L_{\tilde{\rho}_\theta} &= 2 \left\{ \frac{|\dot{\rho}_\theta\rangle\rangle\langle\langle\rho_\theta|}{\text{Tr}(\rho_\theta^2)} + \frac{|\rho_\theta\rangle\rangle\langle\langle\dot{\rho}_\theta|}{\text{Tr}(\rho_\theta^2)} - \frac{d \text{Tr}(\rho_\theta^2)/d\theta}{[\text{Tr}(\rho_\theta^2)]^2} |\rho_\theta\rangle\rangle\langle\langle\rho_\theta| \right\} \\ &= \frac{2}{\text{Tr}(\rho_\theta^2)} (|\dot{\rho}_\theta\rangle\rangle\langle\langle\rho_\theta| + |\rho_\theta\rangle\rangle\langle\langle\dot{\rho}_\theta| - 2\langle\langle\rho_\theta|\dot{\rho}_\theta\rangle\rangle\tilde{\rho}_\theta), \end{aligned} \quad (\text{B1})$$

having used $d \text{Tr}(\rho_\theta^2)/d\theta = 2 \text{Tr}(\rho_\theta \dot{\rho}_\theta) = 2 \langle \rho_\theta | \dot{\rho}_\theta \rangle$. Then we have

$$L_{\tilde{\rho}_\theta}^2 = \frac{4}{[\text{Tr}(\rho_\theta^2)]^2} [\text{Tr}(\rho_\theta^2) \langle \dot{\rho}_\theta | \dot{\rho}_\theta \rangle \tilde{\rho}_\theta - \langle \rho_\theta | \dot{\rho}_\theta \rangle (|\dot{\rho}_\theta \rangle \langle \rho_\theta| + |\rho_\theta \rangle \langle \dot{\rho}_\theta|) + \text{Tr}(\rho_\theta^2) |\dot{\rho}_\theta \rangle \langle \dot{\rho}_\theta|], \quad (\text{B2})$$

which yields

$$\tilde{F}^Q(\tilde{\rho}_\theta) = \text{Tr}(\tilde{\rho}_\theta L_{\tilde{\rho}_\theta}^2) = 4 \left\{ \frac{\langle \dot{\rho}_\theta | \dot{\rho}_\theta \rangle}{\text{Tr}(\rho_\theta^2)} - \left[\frac{\langle \rho_\theta | \dot{\rho}_\theta \rangle}{\text{Tr}(\rho_\theta^2)} \right]^2 \right\}. \quad (\text{B3})$$

□

Appendix C: Proof of Lemma 2

Proof. In general T_θ may or may not be diagonalizable. If T_θ is not diagonalizable, we can add some additional linearly independent vectors $|R_i \rangle$ orthogonal to the subspace of peripheral eigenvectors, such that $\{|R_i \rangle\}_{i=1}^{d^2}$ forms a Jordan basis which spans the whole d^2 -dimensional vector space. Under such choice we have the decomposition $|\rho_0 \rangle = \sum_{i=1}^{d^2} a_i |R_i \rangle$. Without loss of generality, we can always choose a_i to be nonnegative real numbers and $\langle R_i | R_i \rangle = 1$ for all i . By our choice $R_1 = \frac{1}{\sqrt{\text{Tr}(\rho_\theta^2)}} \rho_\theta$ for a fixed point state ρ_θ , and $a_1 = 1/\text{Tr} R_1$. Then we have

$$|\rho_\theta \rangle = T_\theta^N |\rho_0 \rangle = \sum_{i \in S} a_i \lambda_i^N |R_i \rangle, \quad N \rightarrow \infty, \quad (\text{C1})$$

since the N -th power of any Jordan block corresponding to $|\lambda_i| < 1$ converges to 0 as $N \rightarrow \infty$. It follows that

$$|\dot{\rho}_\theta \rangle = \sum_{i \in S} (N a_i \lambda_i^{N-1} \dot{\lambda}_i |R_i \rangle + \dot{a}_i \lambda_i^N |R_i \rangle + a_i \lambda_i^N \dot{R}_i). \quad (\text{C2})$$

Thus we obtain

$$\begin{aligned} \langle \dot{\rho}_\theta | \dot{\rho}_\theta \rangle &= N^2 \sum_{i,j \in S} (\lambda_i^* \lambda_j)^{N-1} a_i a_j \dot{\lambda}_i^* \dot{\lambda}_j \langle R_i | R_j \rangle \\ &\quad + 2N \sum_{i,j \in S} (\lambda_i^* \lambda_j)^{N-1} \dot{\lambda}_i^* \dot{\lambda}_j (\dot{a}_i a_j \langle R_i | R_j \rangle + a_i a_j \langle \dot{R}_i | R_j \rangle) \\ &\quad + \sum_{i,j \in S} (\lambda_i^* \lambda_j)^N (\dot{a}_i \dot{a}_j \langle R_i | R_j \rangle + a_i a_j \langle \dot{R}_i | \dot{R}_j \rangle + \dot{a}_i a_j \langle R_i | \dot{R}_j \rangle + a_i \dot{a}_j \langle \dot{R}_i | R_j \rangle), \end{aligned} \quad (\text{C3})$$

and

$$\langle \rho_\theta | \dot{\rho}_\theta \rangle = N \sum_{i,j \in S} (\lambda_i^* \lambda_j)^{N-1} a_i a_j \dot{\lambda}_i^* \dot{\lambda}_j \langle R_i | R_j \rangle + \sum_{i,j \in S} (\lambda_i^* \lambda_j)^N (a_i \dot{a}_j \langle R_i | R_j \rangle + a_i a_j \langle R_i | \dot{R}_j \rangle), \quad (\text{C4})$$

having used the property that eigenvalues come in complex conjugate pairs. By using Lemma 1 and the relation $\text{Tr}(\rho_\theta^2) = \langle \rho_\theta | \rho_\theta \rangle = \sum_{i,j \in S} (\lambda_i^* \lambda_j)^N a_i a_j \langle R_i | R_j \rangle$, we then obtain Eq. (6). □

Appendix D: Proof of Theorem 1

Proof. Define

$$|D_\theta \rangle := \sum_{i \in S} N a_i \lambda_i^{N-1} \dot{\lambda}_i |R_i \rangle, \quad (\text{D1})$$

which constitutes a part of the contribution to $|\dot{\rho}_\theta \rangle$ in Eq. (C2). Then by Lemma 2 it follows that

$$\lim_{N \rightarrow \infty} \frac{\tilde{F}^Q(\tilde{\rho}_\theta)}{N^2} = \frac{4}{N^2} \left\{ \frac{\langle D_\theta | D_\theta \rangle}{\text{Tr}(\rho_\theta^2)} - \left[\frac{\langle \rho_\theta | D_\theta \rangle}{\text{Tr}(\rho_\theta^2)} \right]^2 \right\}. \quad (\text{D2})$$

By the Cauchy–Schwarz inequality and noting that the QFI is a real number, we have

$$\langle\langle \rho_\theta | D_\theta \rangle\rangle^2 \leq \langle\langle \rho_\theta | \rho_\theta \rangle\rangle \langle\langle D_\theta | D_\theta \rangle\rangle = \text{Tr}(\rho_\theta^2) \langle\langle D_\theta | D_\theta \rangle\rangle, \quad (\text{D3})$$

where the equality holds if and only if $|D_\theta\rangle \propto |\rho_\theta\rangle$. Equivalently this condition can be formulated as $\dot{\lambda}_i/\lambda_i = \dot{\lambda}_j/\lambda_j$ for all $i, j \in \mathbf{S}$ associated with $a_i \neq 0$ and $a_j \neq 0$. When the condition is violated, we can obtain $\lim_{N \rightarrow \infty} \frac{\tilde{F}^Q(\tilde{\rho}_\theta)}{N^2} > 0$ that yields the HL.

Now we denote the fixed point state by ρ_* with the eigenvalue $\lambda_1 = 1$. If there exists some λ_j such that $|\lambda_j| = 1$ and $\dot{\lambda}_j \neq 0$, we will see that it is always possible to choose an input state with $a_1 \neq 0$ and $a_j \neq 0$. By the trace-preserving property of the quantum channel we have $\lim_{\theta \rightarrow \theta_0} \text{Tr} R_j = 0$, so we can take an input state $\rho_0 = (1 - \alpha)I/d + \alpha\rho_* + \beta(R_j + R_j^\dagger)$ for some $\alpha > 0$ and $\beta > 0$. Note that if R_j is proportional to a Hermitian matrix, we have the freedom to simply take R_j to be Hermitian. Since $\dot{\lambda}_1 = 0$ and $\dot{\lambda}_j \neq 0$, this choice of the input state allows for the HL. \square

Appendix E: Proof of Theorem 2

Proof. Our goal is to show that the regulated channel $(U_c \otimes U_c^*)T_\theta$ has a peripheral eigenmatrix R_0 and the associated eigenvalue has a nonzero derivative in the limit of $\theta \rightarrow \theta_0$, even if this may not hold for T_θ itself.

First we will show that $|R_0\rangle \in \mathcal{P}$ is the limit of a peripheral eigenvector of $(U_c \otimes U_c^*)T_\theta$. Denoting by μ_0 the eigenvalue of $T_\theta^\dagger \dot{T}_\theta$ associated with R_0 , we have

$$\mu_0 |R_0\rangle = \lim_{\theta \rightarrow \theta_0} T_\theta^\dagger \dot{T}_\theta |R_0\rangle = T_{\theta_0}^\dagger \lim_{d\theta \rightarrow 0} \frac{T_{\theta_0+d\theta} - T_{\theta_0}}{d\theta} |R_0\rangle = T_{\theta_0}^\dagger (U_c^\dagger \otimes U_c^T)(U_c \otimes U_c^*) \lim_{d\theta \rightarrow 0} \frac{T_{\theta_0+d\theta} - T_{\theta_0}}{d\theta} |R_0\rangle, \quad (\text{E1})$$

so for $d\theta \rightarrow 0$ we obtain $(U_c \otimes U_c^*)T_{\theta_0+d\theta}|R_0\rangle \propto |R_0\rangle$, by noting that $T_{\theta_0}^\dagger (U_c^\dagger \otimes U_c^T)|R_0\rangle = |R_0\rangle$ and $(U_c \otimes U_c^*)T_{\theta_0}|R_0\rangle = |R_0\rangle$. Indeed, R_0 is the limit of a peripheral eigenmatrix of $(U_c \otimes U_c^*)T_\theta$.

Then we will show that for any peripheral eigenvalue λ_j of $(U_c \otimes U_c^*)T_\theta$ with the normalized eigenvector $|R_j\rangle$, we have $\lambda_j^* \dot{\lambda}_j = \langle\langle R_j | T_\theta^\dagger \dot{T}_\theta | R_j \rangle\rangle$. By taking derivatives on both sides of $(U_c \otimes U_c^*)T_\theta |R_j\rangle = \lambda_j |R_j\rangle$ we obtain

$$(U_c \otimes U_c^*)\dot{T}_\theta |R_j\rangle + (U_c \otimes U_c^*)T_\theta |\dot{R}_j\rangle = \dot{\lambda}_j |R_j\rangle + \lambda_j |\dot{R}_j\rangle. \quad (\text{E2})$$

It follows that

$$\langle\langle R_j | T_\theta^\dagger \dot{T}_\theta | R_j \rangle\rangle + \langle\langle R_j | T_\theta^\dagger T_\theta | \dot{R}_j \rangle\rangle = \langle\langle R_j | \lambda_j^* \dot{\lambda}_j | R_j \rangle\rangle + \langle\langle R_j | \lambda_j^* \lambda_j | \dot{R}_j \rangle\rangle. \quad (\text{E3})$$

Note that $\langle\langle R_j | T_\theta^\dagger T_\theta | R_j \rangle\rangle = \langle\langle R_j | R_j \rangle\rangle$ since $|R_j\rangle \in \mathcal{P}$. Then we obtain $\lambda_j^* \dot{\lambda}_j = \langle\langle R_j | T_\theta^\dagger \dot{T}_\theta | R_j \rangle\rangle$.

$PT_\theta^\dagger \dot{T}_\theta P \neq 0$ thus implies the existence of some $\dot{\lambda}_j \neq 0$. In particular, R_0 is such an eigenmatrix of $PT_\theta^\dagger \dot{T}_\theta P$ with eigenvalue $\mu_0 = \lambda_0^* \dot{\lambda}_0$. Finally, by Theorem 1 the repeated application of $(U_c \otimes U_c^*)T_\theta$ can achieve the HL. \square

Appendix F: Algorithm for identification of the unitary control

In Algorithm 1, we delineate in detail the procedure for identifying the unitary control in Theorem 2 for achieving the HL. The code implementation is openly available on GitHub [41].

Proof. First, it is easy to see that the existence of a unitary transformation between two sets of Hermitian matrices is equivalent to the existence of a unitary transformation between two sets of subspaces, if we apply the spectral decomposition to each Hermitian matrix. Denote by $\{P_1, \dots, P_K\}$ the subspaces generated by the spectral decomposition of all matrices in $\{R_i\}_{i=1}^2$, and by $\{Q_1, \dots, Q_K\}$ the subspaces generated by the spectral decomposition of all matrices in $\{\sum_k K_k^{\theta_0} R_i K_k^{\theta_0^\dagger}\}_{i=1}^2$.

We start from the characterization of the principal angles between two subspaces F and G . It is always possible to choose a set of orthonormal basis vectors $V_F = \{|u_1\rangle, \dots, |u_\alpha\rangle, |v_1\rangle, \dots, |v_\beta\rangle, |\psi_1\rangle, \dots, |\psi_\gamma\rangle\}$ for F and a set of orthonormal basis vectors $V_G = \{|u'_1\rangle, \dots, |u'_\alpha\rangle, |w_1\rangle, \dots, |w_\beta\rangle, |\phi_1\rangle, \dots, |\phi_\delta\rangle\}$ for G , such that any vector in the set V_F and any vector in the set V_G are orthogonal, except for

$$\langle v_i | w_i \rangle = \cos(\eta_i), \quad \forall i = 1, \dots, \beta \quad (\text{F1})$$

Algorithm 1: Identification of a unitary control U_c in Theorem 2.

Input: R_0 in Eq. (8)
Output: Unitary control U_c
 $R_1 \leftarrow R_0 + R_0^\dagger$, $R_2 \leftarrow i(R_0 - R_0^\dagger)$
 $\text{List}_{\text{in}} \leftarrow [R_1, R_2]$, $\text{List}_{\text{out}} \leftarrow [\sum_k K_k^{\theta_0} R_1 K_k^{\theta_0^\dagger}, \sum_k K_k^{\theta_0} R_2 K_k^{\theta_0^\dagger}]$
 $\text{Vectors}_{\text{in-out}} \leftarrow []$ /* To store two sets of vectors connected by a unitary transformation U_c^\dagger */
for List **in** $[\text{List}_{\text{in}}, \text{List}_{\text{out}}]$ **do**
 for $j \leftarrow 1$ **to** 2 **do**
 $R \leftarrow \text{List}[j]$
 Spectral decomposition $R = \sum_{k=1}^{n_\Pi} \alpha_k \Pi_k$, where $\Pi_k = \sum_{a=1}^{n_v^{(k)}} |v_{ka}\rangle\langle v_{ka}|$ /* $\{\Pi_k\}_k$ is a set of projections; α_k are different for different k and follow the descending order */
 $S_k \leftarrow [|v_{k1}\rangle, \dots, |v_{kn_v^{(k)}}\rangle]$, $\forall k = 1, \dots, n_\Pi$ /* S_k is a subspace spanned by orthonormal $\{|v_{ka}\rangle\}_a$ */
 $\mathcal{S}_j \leftarrow [S_1, \dots, S_{n_\Pi}]$ /* \mathcal{S}_j is a list of subspaces corresponding to R */
 $\mathcal{S} \leftarrow \bigcup_{j=1}^m \mathcal{S}_j$ /* \mathcal{S} is the union of all subspaces */
 repeat
 for every pair of S_x, S_y **in** \mathcal{S} **do**
 Π_x, Π_y are the projections on S_x, S_y
 Compute the SVD of $\Pi_x \Pi_y = U D V^\dagger$
 Obtain a list of subspaces $[X_1, \dots, X_{n_s}]$, each spanned by the column vectors of U corresponding to the same *nonzero* singular value in the ascending order
 Obtain a list of subspaces $[Y_1, \dots, Y_{n_s-1}]$, each spanned by the row vectors of V^T corresponding to the same *nonzero and nonunity* singular value in the ascending order
 X_{n_s+1} is the orthogonal complement to X_1, \dots, X_{n_s} in S_x and Y_{n_s} is the orthogonal complement to Y_1, \dots, Y_{n_s-1} in S_y
 $S_{xy} \leftarrow [X_1, \dots, X_{n_s+1}, Y_1, \dots, Y_{n_s}]$ /* The angles between S_x, S_y are uniquely mapped to angles between subspaces in S_{xy} */
 $\mathcal{S} \leftarrow \bigcup_{x,y} S_{xy}$
 Remove redundant subspaces in \mathcal{S} if they are associated with identical projections
 until for every pair of subspaces S_a, S_b in \mathcal{S} with projections Π_a, Π_b , either $\Pi_a \Pi_b = 0$, or Π_a and Π_b have the same rank and all nonzero singular values of $\Pi_a \Pi_b$ are the same
 $\mathcal{S}' \leftarrow []$ /* \mathcal{S}' is to store subspaces with basis vectors in a uniquely determined canonical order */
 repeat
 Add the first subspace S_1 in \mathcal{S} to \mathcal{S}' and remove S_1 from \mathcal{S}
 Find all the remaining subspaces Q_1, \dots, Q_L in \mathcal{S} which are not orthogonal to S_1 , and remove them from \mathcal{S}
 for $j \leftarrow 1$ **to** L **do**
 Π_1, Γ_j are rank- n_j projections on S_1, Q_j
 Construct isometry \tilde{U} with each column as a basis vector in subspace S_1
 $\tilde{V}^\dagger \leftarrow \tilde{D}^{-1} \tilde{U}^\dagger \Pi_1 \Gamma_j$, where \tilde{D} is diagonal with all diagonal elements as the nonzero singular value of $\Pi_1 \Gamma_j$
 $Q_j \leftarrow [|v_1\rangle, \dots, |v_{n_j}\rangle]$, where $|v_1\rangle, \dots, |v_{n_j}\rangle$ are the row vectors of \tilde{V}^T
 Add Q_j to \mathcal{S}' and remove Q_j from \mathcal{S}
 until \mathcal{S} is empty
 $\text{List}_{\text{vectors}} \leftarrow []$
 Add all the basis vectors of all the subspaces in \mathcal{S}' to $\text{List}_{\text{vectors}}$, following the order established so far
 Add $\text{List}_{\text{vectors}}$ to $\text{Vectors}_{\text{in-out}}$
For $i = 1, 2$, construct matrices M_i , with each column as a basis vector in $\text{Vectors}_{\text{in-out}}[i]$ following the established order
Compute the SVD of $M_2 M_1^\dagger = U' D' V'^\dagger$
 $U_c \leftarrow V' U'^\dagger$ /* U_c^\dagger maps vectors in $\text{Vectors}_{\text{in-out}}[1]$ to vectors in $\text{Vectors}_{\text{in-out}}[2]$ */
Sanity check: If Eq. (8) is satisfied by U_c , output U_c and succeed; otherwise, there does not exist a unitary satisfying Eq. (8).

and

$$\langle u_i | u'_i \rangle = 1, \quad \forall i = 1, \dots, \alpha, \quad (\text{F2})$$

where $0 < \eta_i < \pi/2$ are nontrivial principal angles. We say this is a canonical order of basis vectors for these two subspaces F and G . These principal angles can be determined by performing the SVD of $\Pi_F \Pi_G$, as $\cos(\eta_j)$ is the singular value. By the uniqueness of SVD, $\{|u_i\rangle = |u'_i\rangle\}_{i=1}^\alpha$ are unique up to a unitary transformation, $\{|v_j\rangle\}$ and $\{|w_j\rangle\}$ associated with the same η_j are unique up to a simultaneous unitary transformation, $\{\psi_i\}_{i=1}^\gamma$ are unique up to a unitary transformation, and $\{\phi_i\}_{i=1}^\delta$ are unique up to a unitary transformation. The geometrical relation between

two subspaces F and G are thus fully characterized by the angles between a set of lower-dimensional subspaces.

Iteratively, we repeat the procedure of reducing the dimensions of subspaces, for all pairs of subspaces in the set $\{P_1, \dots, P_K\}$, until any pair of the dimension-reduced subspaces are either mutually orthogonal or have the same dimensions and identical principal angles. Denote by $\{\tilde{P}_1, \dots, \tilde{P}_M\}$ this set of subspaces iteratively obtained so far. We then fix a canonical order of basis vectors for all these subspaces through such a procedure: we first choose an order of basis vectors for subspace \tilde{P}_1 with the associated projection $\tilde{\Pi}_1$. Then for any subspace \tilde{P}_j (with the projection $\tilde{\Pi}_j$) in $\{\tilde{P}_2, \dots, \tilde{P}_M\}$ which is nonorthogonal to \tilde{P}_1 , the canonical order of basis vectors is uniquely determined by fixing the isometry \tilde{U} in the SVD of $\tilde{P}_1 \tilde{\Pi}_j = \tilde{U} \tilde{D} \tilde{V}^\dagger$, where the diagonal elements of \tilde{D} only contain nonzero singular values. We can thus choose $\tilde{V}^\dagger = \tilde{D}^{-1} \tilde{U}^\dagger \tilde{P}_1 \tilde{\Pi}_j$, where each column of \tilde{U} is the predetermined canonical basis vector for subspace $\tilde{\Pi}_1$. After finding all subspaces P_j nonorthogonal to P_1 , we simply fix the order of basis vectors for another subspace in the remaining set of unchosen subspaces and repeat the process. Therefore, we find a set of basis vectors uniquely determined, and we can construct a matrix M_1 , whose columns are these basis vectors in this canonical order. In the same way, we can also reduce the dimensions for subspaces in $\{Q_1, \dots, Q_K\}$, find a corresponding set of basis vectors and construct matrix M_2 .

Finally, we would like to find a unitary U_c such that $U_c^\dagger M_1 = M_2$. This can be easily done, by computing the SVD of $M_2 M_1^\dagger = U' D' V'^\dagger$ and choose $U_c = V' U'^\dagger$. One way to see this is that U_c^\dagger is the solution to the unitary Procrustes problem $\arg \min_U \|U M_1 - M_2\|_2^2$ [42]. Such U_c exists if and only if the inner products between column vectors of M_1 are identical to the inner products between column vectors of M_2 . Tracing back the iterative reduction and considering the uniqueness of the canonical choice, if these inner products are preserved, then $U_c^\dagger P_i U_c = Q_i$, $\forall i = 1, \dots, K$, and therefore U_c is a solution of Eq. (8). In turn, if a unitary satisfying Eq. (8) exists, it must preserve all these inner products by construction. Therefore, U_c satisfying Eq. (8) exists if and only if Algorithm 1 can successfully identify it. \square

Appendix G: Proof of Theorem 3

Proof. Without loss of generality, we consider the case where $U_{\theta_0} = V_{\theta_0} = I$; otherwise, a unitary control $U_{\theta_0}^\dagger V_{\theta_0}^\dagger$ can be appended to T_θ . We further choose a basis of linearly independent n -qubit Pauli operators (including the identity) $\{P'_1, P'_2, \dots, P'_s\}$ in $\text{Span}\{\langle P_1, P_2, \dots, P_r \rangle\}$ for $s \geq r$. Obviously, we have $\text{Span}\{\langle P_1, P_2, \dots, P_r \rangle\} = \text{Span}\{P'_1, P'_2, \dots, P'_s\}$.

As under our assumption T_{θ_0} is an n -qubit Pauli channel, the projection P on the subspace \mathcal{P} of eigenvectors of $T_\theta^\dagger T_\theta$ with eigenvalues 1 can be expressed by

$$P = \prod_{i=1}^r \left[\frac{1}{2} (I + K_i^\theta \otimes K_i^{\theta*}) \right] = \prod_{i=1}^r \left[\frac{1}{2} (I + P_i \otimes P_i^*) \right] = \prod_{i=1}^s \left[\frac{1}{2} (I + P'_i \otimes P_i'^*) \right]. \quad (\text{G1})$$

It is worth mentioning that all $P'_i \otimes P_i'^*$ commute with each other, so the order in the product does not matter. Besides, in this case \mathcal{P} is also the subspace of peripheral eigenvectors of T_{θ_0} itself, so the second condition Eq. (8) in Theorem 2 is naturally satisfied with trivial identity control $U_c = U_{\theta_0}^\dagger V_{\theta_0}^\dagger = I$.

We now check the first condition Eq. (7) in Theorem 2, by evaluating (at $\theta = \theta_0$)

$$\begin{aligned} P T_\theta^\dagger \dot{T}_\theta P &= -i P T_\theta^\dagger T_\theta [H^{(U)} \otimes I - I \otimes H^{(U)*}] P - i P T_\theta^\dagger [H^{(V)} \otimes I - I \otimes H^{(V)*}] T_\theta P \\ &= -i \frac{1}{2^{2s}} (I + P'_s \otimes P_s'^*) \cdots (I + P'_1 \otimes P_1'^*) T_\theta^\dagger T_\theta [H^{(U)} \otimes I - I \otimes H^{(U)*}] (I + P'_1 \otimes P_1'^*) \cdots (I + P'_s \otimes P_s'^*) \\ &\quad - i \frac{1}{2^{2s}} (I + P'_s \otimes P_s'^*) \cdots (I + P'_1 \otimes P_1'^*) T_\theta^\dagger [H^{(V)} \otimes I - I \otimes H^{(V)*}] T_\theta (I + P'_1 \otimes P_1'^*) \cdots (I + P'_s \otimes P_s'^*) \quad (\text{G2}) \\ &= -i \frac{1}{2^{2s}} (I + P'_s \otimes P_s'^*) \cdots (I + P'_1 \otimes P_1'^*) (H_{\text{tot}} \otimes I - I \otimes H_{\text{tot}}^*) (I + P'_1 \otimes P_1'^*) \cdots (I + P'_s \otimes P_s'^*) \\ &= -i \frac{1}{2^{2s}} \sum_k \alpha_k [(I + P'_s \otimes P_s'^*) \cdots (I + P'_1 \otimes P_1'^*) (Q_k \otimes I - I \otimes Q_k^*) (I + P'_1 \otimes P_1'^*) \cdots (I + P'_s \otimes P_s'^*)]. \end{aligned}$$

, having used $H^{(U)} = i U_\theta^\dagger \dot{U}_\theta$, $H^{(V)} = i V_\theta^\dagger \dot{V}_\theta$ and $H_{\text{tot}} = H^{(U)} + H^{(V)} = \sum_k \alpha_k Q_k$. For any n -qubit Pauli operator P'_i and any n -qubit Pauli operator Q_k , if $\{Q_k, P'_i\} = 0$, then

$$(I + P'_i \otimes P_i'^*) (Q_k \otimes I - I \otimes Q_k^*) (I + P'_i \otimes P_i'^*) = 0; \quad (\text{G3})$$

if $Q_k = P'_i$, then Eq. (G3) also holds. However, if $[Q_k, P'_i] = 0$, then

$$(I + P'_i \otimes P_i'^*) (Q_k \otimes I - I \otimes Q_k^*) (I + P'_i \otimes P_i'^*) = 2Q_k \otimes I + 2Q_k P'_i \otimes P_i'^* - 2I \otimes Q_k^* - 2P'_i \otimes (Q_k P'_i)^*. \quad (\text{G4})$$

Note that, for any $i = 1, \dots, s$, if $Q_k \notin \text{Span}\{P'_1, P'_2, \dots, P'_s\}$, then $Q_k P'_i \notin \text{Span}\{P'_1, P'_2, \dots, P'_s\}$. Combining it with Eq. (G4) and requiring $[Q_k, P'_i] = 0$ for $i = 1, \dots, s$ (or equivalently, $[Q_k, P_i] = 0$ for $i = 1, \dots, r$), each term in the summation over k in the last line of Eq. (G2) does not vanish, and in particular, contains Pauli terms $Q_k \otimes I - I \otimes Q_k^*$ (up to a multiplicative factor). Furthermore, in the summation over different k in Eq. (G2), such Pauli terms cannot cancel each other as $\{Q_k\}$ are linearly independent. Therefore, we prove that $PT_\theta^\dagger \dot{T}_\theta P \neq 0$. Finally, by applying Theorem 2 we complete the proof. \square

Appendix H: Supplemental examples

1. The singularity of HNKs condition

We first consider a simple but illuminating example, which reveals some subtle issues not captured by the HNKs condition, but made explicit by our theoretical framework. In fact this issue arises from the ill-defined ‘‘Hamiltonian’’ in certain cases.

Suppose we want to estimate θ from N queries to a σ_z -rotation under the single qubit dephasing noise, described by Kraus operators $K_1 = \sqrt{1-p}e^{-i\phi\sigma_z/2}$ and $K_2 = \sqrt{p}\sigma_z e^{-i\phi\sigma_z/2}$. Both p and ϕ are functions of the parameter of interest θ . This specific problem is of fundamental interest in the asymptotic theory of quantum channel estimation, because any quantum channel can simulate a logical dephasing channel by using error correction (with ancilla in general) [21].

Ref. [21, Eq. (B5)] showed that this channel has a ‘‘Hamiltonian’’ independent of p : $H = i\sum_j K_j^\dagger \dot{K}_j = \frac{\dot{\phi}}{2}\sigma_z$. The authors therefore concluded that HL can only be achieved when (i) $\dot{\phi} \neq 0$ and (ii) $p = 0$ or 1 , according to the HNKs condition. However, our analysis shows that HL can also be achieved if (i) $\dot{p} \neq 0$ and (ii) $p = 0$ or 1 . Specifically, $T_\theta = \sum_i K_i \otimes K_i^*$ has 4 eigenvalues: $\{1, 1, (1-2p)e^{-i\phi}, (1-2p)e^{i\phi}\}$, and the eigenvectors are mutually orthogonal. For $\lambda = (1-2p)e^{i\phi}$ we have $\dot{\lambda}|_{p=0} = (i\dot{\phi} - 2\dot{p})e^{i\phi}$ and $\dot{\lambda}|_{p=1} = (-i\dot{\phi} - 2\dot{p})e^{i\phi}$, so by Theorem 1 we can choose an input state $\rho_0 = I/2 + \alpha(|0\rangle\langle 1| + |1\rangle\langle 0|)$ (for some $0 < \alpha < 1/2$) which achieves the HL when (i) $p = 0$ or 1 and (ii) either $\dot{\phi} \neq 0$ or $\dot{p} \neq 0$.

2. HL without decoherence-free subspace

Existing QEC protocols achieving the HL construct a DFS, which constructs a DFS, where the noise is eliminated but the signal remains to take effect. By QEC the simulated channel is an identity channel on the logical subspace at $\theta = \theta_0$ [21]. Our analysis, however, opens up new possibilities to achieve the HL without constructing the DFS.

Consider N queries to a quantum channel described by Kraus operators $K_1 = |2\rangle\langle 0|$, $K_2 = |2\rangle\langle 1|$, $K_3 = \sqrt{2\theta}|2\rangle\langle 2|$, $K_4 = \sqrt{1/2 - \theta}|0\rangle\langle 2|$, and $K_5 = \sqrt{1/2 - \theta}|1\rangle\langle 2|$, where $0 \leq \theta \leq 1/2$ is the parameter of interest. Now $T_\theta = \sum_i K_i \otimes K_i^*$ has 2 nonzero eigenvalues: $\{1, -1 + 2\theta\}$, with the fixed point $\text{diag}\{1/2 - \theta, 1/2 - \theta, 1\}$ and the other eigenmatrix $\text{diag}\{1/2, 1/2, -1\}$ (where $\text{diag}\{a_i\}_i$ denotes a diagonal matrix with diagonal elements $\{a_i\}_i$). At $\theta = 0$, we can choose an input state $\rho_0 = \text{diag}\{1/4, 1/4, 1/2\} + \alpha \text{diag}\{1/4, 1/4, -1/2\}$ for some $-1 < \alpha < 1$ and $\alpha \neq 0$. Here these two eigenvectors are not orthogonal. By Lemma 2, the associated QFI of the asymptotic output state at $\theta = 0$ exhibits an interesting oscillating behaviour given by

$$\lim_{N \rightarrow \infty} \frac{\tilde{F}^Q(\tilde{\rho}_\theta)}{N^2} = \begin{cases} \frac{128\alpha^2}{(3\alpha^2 + 2\alpha + 3)^2}, & \text{if } N \text{ is odd,} \\ \frac{128\alpha^2}{(3\alpha^2 - 2\alpha + 3)^2}, & \text{if } N \text{ is even.} \end{cases} \quad (\text{H1})$$

The QFI of the output state is lower bounded by

$$\lim_{N \rightarrow \infty} \frac{F^Q(\rho_\theta)}{N^2} \geq \lim_{N \rightarrow \infty} \frac{\text{Tr}(\rho_\theta^2)}{4\lambda_{\max}(\rho_\theta)N^2} \tilde{F}^Q(\tilde{\rho}_\theta) = \begin{cases} \frac{8\alpha^2}{(3\alpha^2 + 2\alpha + 3)(1+\alpha)}, & \text{if } N \text{ is odd,} \\ \frac{16\alpha^2}{(3\alpha^2 - 2\alpha + 3)(1+\alpha)}, & \text{if } N \text{ is even,} \end{cases} \quad (\text{H2})$$

when $1/3 < \alpha < 1$. However, Eq. (H2) only gives a lower bound on the actual QFI, so it is unclear whether the QFI also oscillates with N asymptotically. We compute the exact QFI for this example, and find that this oscillating behaviour indeed exists for fairly large N , as illustrated in Fig. 3. Since N is a finite number in a realistic scenario, we anticipate that this phenomenon may be of practical interest and deserves further investigation.

Furthermore, we remark that this quantum channel is irreducible, i.e., having a unique full-rank fixed point, and does not admit a DFS. The HL here is therefore not a result of DFS, but stems from the decay of root-of-unity

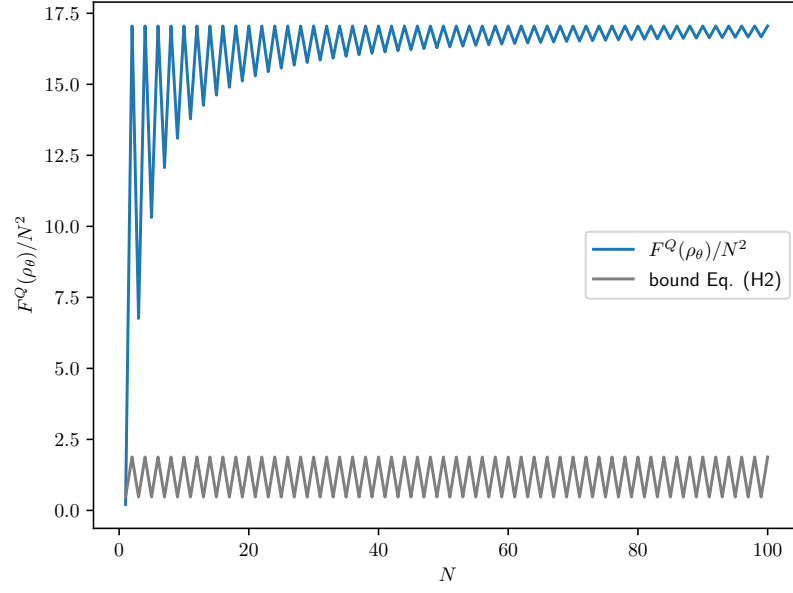


FIG. 3. Comparison between the actual normalized QFI $F^Q(\rho_\theta)/N^2$ and the bound Eq. (H2). The input state is a fixed state $\rho_0 = \text{diag}\{1/4, 1/4, 1/2\} + \alpha \text{diag}\{1/4, 1/4, -1/2\}$ for $\alpha = 0.9$.

peripheral eigenvalues corresponding to diagonalizable conserved quantities [38]. It is worth noting that the HNKS condition is also ill-defined for this example.